Biol. Cybern. 90, 256–263 (2004)
DOI 10.1007/s00422-004-0472-8

Biological Cybernetics

Perceptual dominance time distributions in multistable visual perception

Y. H. Zhou[1], J. B. Gao[1], K. D. White[2], I. Merk[3], K. Yao[4]

[1] Department of Electrical and Computer Engineering, EB 559, University of Florida, Gainesville, FL 32611, USA
[2] Department of Psychology, University of Florida, P.O. Box 112250, Gainesville, FL 32611-2250, USA
[3] Gerling Global Reinsurance Company, Cologne, Germany
[4] Department of Electrical Engineering, University of California, Los Angeles, CA 90095, USA

Received: 28 April 2003 / Accepted: 2 February 2004 / Published online: 31 March 2004

Abstract. Perceptual multistability, alternative perceptions of an unchanging stimulus, gives important clues to neural dynamics. The present study examined 56 perceptual dominance time series for a Necker cube stimulus, for ambiguous motion, and for binocular rivalry. We made histograms of the perceptual dominance times, based on from 307 to 2478 responses per time series (median = 612), and compared these histograms to gamma, lognormal and Weibull fitted distributions using the Kolmogorov–Smirnov goodness-of-fit test. In 40 of the 56 tested cases a lognormal distribution provided an acceptable fit to the histogram (in 24 cases it was the only fit). In 16 cases a gamma distribution, and in 11 cases a Weibull distribution, were acceptable but never as the only fit in either case. Any of the three distributions were acceptable in three cases and none provided acceptable fits in 12 cases. Considering only the 16 cases in which a lognormal distribution was rejected ($p < 0.05$) revealed that minor adjustments to the fourth-moment term of the lognormal characteristic function restored good fits. These findings suggest that random fractal theory might provide insight into the underlying mechanisms of multistable perceptions.

1 Introduction

Few images are as fascinating as those whose appearances change spontaneously (Attneave 1971). That is, during continuous observation of an unchanging stimulus, the perceptual system will first adopt one and sometime later another interpretation, switching over time between alternative dominant percepts. This can be demonstrated using the classical Necker cube shown in Fig. 1a. Multistable visual perception, such as of the Necker cube, is a phenomenon that intrigued scientists for centuries. For example, psychologists have performed numerous experiments with the Necker cube to explore the effects of contrast, luminance, completeness, size, base angle, use of a fixation point, interpolation of squares or cubes, and varying the side-to-base ratio of the stimuli, as well as subject-related variables such as experience, gender, volitional control, attention, or heat and noise in the environment (see review by Merk and Schnakenberg 2002). The significance of research on multistable perception is that it can offer a starting point to investigate consciousness (Crick and Koch 1990) as well as visual information processing, perceptual organization, and the transition from sensation to perception (Blake and Logothetis 2002).

Conventional explanations of multistable visual phenomena suggest that the spontaneous perceptual switches are due to antagonistic connectivity within the visual system (Leopold and Logothetis 1999). A prime example of this is binocular rivalry, a form of interocular competition that arises when patterns in the two eyes cannot be fused stereoscopically (see Fig. 1b and c). Recent electrophysiological and functional imaging studies reveal important clues to the origins of visual multistability during binocular rivalry in striate, extrastriate, parietal, temporal, and possibly even frontal cortex (Elbert et al. 1985; Lumer et al. 1998; von Steinbüchel 1998; Tong et al. 1998; Inui et al. 2000; Sengpeil 2000; Leopold et al. 2002; Sterzer et al. 2002; White et al. 2002).

The dynamics of alternating perceptual dominance has also offered clues about the underlying mechanisms. The dominance times are irregular and rather unpredictable, so that they need to be described by their statistical properties. Since the classic work of Borsellino et al. (1972) on gamma distribution of experimental perceptual dominance time series researchers have generally compared their experimental data or theoretical model results with gamma distributions, e.g., experiments by Gómez et al. (1995), Pettigrew and Miller (1998), and Vetter et al. (2000) and models by Ditzinger and Haken (1990), Haken (1994), Nagao et al. (2000), Otterpohl et al. (2000), Wilson et al. (2000), and Laing

Correspondence to: J. B. Gao
(e-mail: gao@ece.ufl.edu)

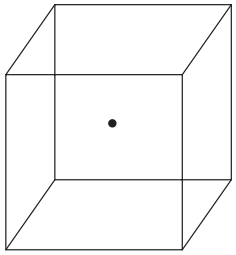

(a) Necker cube

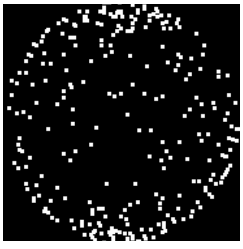

(b) Turning ball (one frame)

(c) Standard binocular rivalry

Fig. 1. Schematic stimuli that generated the multistable perceptions

and Chow (2002). The gamma distribution is related to Poisson processes in which the numbers of changes in nonoverlapping intervals are independent for all intervals. Recently, however, Merk and Schnakenberg (2002) found that the gamma distribution did not pass chi-square tests against their data. Lehky (1995) demonstrated that binocular rivalry is not chaotic and dominance durations in binocular rivalry had a lognormal distribution. Kruse et al. (1996) showed that percepts of stroboscopic alternative motions, including fluttering motion, turning motion, and oppositional motion, have lognormal distributions. These papers encouraged us to continue our research. In the event that a lognormal distribution can fit the present perceptual dominance data for several multistable perception, it encourages the application of multifractal theory to investigate self-similarities (possibly long-range correlations) in the underlying time series (Bershadskii et al. 2001; Gao et al. 2003).

In the present paper, the gamma, lognormal and Weibull distributions will be compared to observed perceptual dominance time series histograms using statistical goodness-of-fit tests. Four groups of perceptual dominance time series will be analyzed. One group represents changing apparent depth relationships of the Necker cube (11 cases). A second group of 7 cases represents time series for the changing apparent motion directions of a "turning ball" stimulus (Bonneh and Gepshtein 2001), and the remaining two groups represent binocular rivalry time series either with orthogonal gratings (27 cases) or orthogonally oriented "turning balls" (11 cases) used as the stimuli.

2 Experiment brief

For one experiment, a Necker cube as shown in Fig. 1a was placed in the middle of a computer screen displayed as black lines on a white background with a visual subtense angle of 4°. A small spot in the middle of the cube served as the fixation point. Subjects drawn from a group of unpaid volunteers were instructed to press a key on the computer keyboard in front of them each time their perception of the cube changed its 3D orientation. The overall observation time was 50 min, consisting of ten runs of 5 min each. The runs were interrupted by breaks of a length freely chosen by the subjects to minimize fatigue effects.

For a second experiment a "turning ball" stimulus, described by Bonneh and Gepshtein (2001), was placed in the middle of a computer screen displayed as white dots on a black background with a visual subtense angle of 4.5°. A single frame from the 120-frame animation (presented at 60 frames per second) is illustrated in reverse contrast in Fig. 1b. A small black X in the middle of the ball, not visible on this figure, served as the fixation point. Subjects pressed a key on the computer keyboard to indicate their perception of the direction of the ball's apparent rotation. The overall observation time was 48 min, consisting of 15 runs of 3.2 min each. The runs were interrupted by breaks of a length freely chosen by the subjects.

The binocular rivalry experiments were more involved. The horizontal or vertical square-wave grating images, as shown in Fig. 1c, were respectively drifting vertically or horizontally. They were displayed in alternate video frames at the middle of the computer screen. Liquid crystal shutter glasses were synchronized to the frame rate, alternately exposing the display to the two eyes at the same frequency as the display frame rate, so that one orientation of grating was presented to only one eye and the other orientation only to the other eye. Due to the rapid shuttering and persistence of our perceptual system, each eye will fuse its successive images into an apparently continuous smoothly moving grating. When both eyes view the orthogonal gratings, the resulting perceptual experience typically is of unpredictable switches between the mutually exclusive perceptions: a second or more seeing only the horizontal grating, then a second or more seeing only the vertical grating. A 2°-disk filled with 2.5 -cycle -per -degree horizontal grating drifting two cycles per second was presented to the right eye while a similar vertical grating was presented to the left eye (or vice versa). Both eyes continuously viewed ample binocular fixation guides. In one experiment the subjects pressed mouse buttons to indicate their perceptual state. On each of 2 days, these 9 subjects performed 14 2-min runs, with rests between runs at the subjects' discretion. In total 18 data sets of 28 min each were obtained in this experiment. In a second experiment 8 subjects pressed keys on a keyboard to indicate their perceptual state. These subjects performed 15 runs of 3.2 min each, with rests between runs at the subjects' discretion. In total nine data sets of 48 min each were obtained (one subject participated twice, on separate

days). The dominance periods (time interval) were extracted for each reported dominant percept, horizontal or vertical, from all of the data sets.

Lastly, subjects who had judged the "turning ball" stimulus as described above also participated in an additional binocular rivalry experiment, but in these runs the orthogonal grating stimuli were replaced by orthogonally oriented "turning ball" stimuli. Subjects pressed a key on the computer keyboard to indicate their perception of the direction of the ball's apparent rotation, which could have been up or down as well as left or right. The overall observation time was 48 min, consisting of 15 runs of 3.2 min each. The runs were interrupted by rests at the subject's discretion, as usual.

3 Parameter estimation for the theoretical probability distributions

Recall that the gamma distribution has previously been used to model binocular rivalry and other perceptual dominance time series (see review by Blake and Logothetis 2002). Its probability density function (pdf) is given by

$$f(x) = \frac{1}{a^b \Gamma(b)} x^{b-1} \mathrm{e}^{-x/a} \quad \text{for } x \geq 0,\ a > 0,\ b > 0 \ , \quad (1)$$

where $\Gamma(b)$ is the gamma function at b. The parameters a and b can be estimated for each sample data set by $a = \sigma^2/\mu$ and $b = \mu/a$, where μ, σ are the mean and the standard deviation of the random variable x (perceptual dominance times), respectively.

The Weibull distribution is one of the most commonly used distributions in reliability engineering. One preferred pdf form of two-parameter Weibull distribution can be expressed by

$$f(x) = abx^{b-1} \mathrm{e}^{-ax^b} \quad \text{for } x \geq 0,\ a > 0,\ b > 0 \ . \quad (2)$$

One robust way to estimate the parameters is to fit each sample data set with the straight line relationship (in log–log coordinates) given by

$$\ln(-\ln(1 - F(x))) = b \ln x + \ln a \ , \quad (3)$$

where $F(x)$ is the cumulative distribution function (CDF). As we can see, b is the slope of the line and $\ln a$ is its intercept at the y-axis. For b greater than unity the pdf of a Weibull function is unimodal, and for $b < 2.6$ the pdf is positively skewed (i.e., a long right tail).

The lognormal distribution also occurs in practice quite often. Its pdf is given by

$$f(x) = \frac{1}{\sqrt{2\pi}\sigma x} \mathrm{e}^{-(\ln x - \mu)^2/2\sigma^2} \quad \text{for } x > 0 \ , \quad (4)$$

where μ, σ are, respectively, the mean and the standard deviation of the logarithm of random variable x for $x > 0$. A straight-line relationship such as (3) can be derived to check the fitness of lognormal distribution as

$$\mathrm{erf}^{-1}(2 * F(x) - 1) = (\ln x - \mu)/\sqrt{2}\sigma \ , \quad (5)$$

where erf is the error function.

Confidence limit formulae for these parameter estimates can be found in Kennedy and Neville (1986) and Miller and Freund (1985). It is worth pointing out that maximum likelihood estimation iterations sometimes showed poor convergence when a sample data set was quite dissimilar from one of these theoretical distributions under consideration. That might also indicate that the chosen distribution could not fit well the measured data.

4 Goodness-of-fit between observations and theoretical distributions

Given the chosen theoretical distribution with its parameters estimated for a particular data set, we determined whether the data plausibly could have arisen from that distribution by performing a goodness-of-fit test. For continuous-time data as a function of a single variable, such as the perceptual dominance times, the preferred test is the Kolmogorov–Smirnov one-sample test (Siegel 1956). The Kolmogorov–Smirnov one-sample test is based on the maximum deviation of the empirical cumulative distribution function from the theoretical one, for each data set and each candidate distribution. The values of a particular empirical CDF, $F(x_i)$, equal i/N, where i is the number of data points not larger than x_i and N is the total number of data points, determined after the dominance times (x) in that data set have been sorted into ascending order.

Corresponding theoretical CDFs, $F_t(x_i)$, were calculated for each candidate distribution with its parameters estimated for that particular data set. The test statistic is the maximum discrepancy between the empirical and theoretical CDFs across all data points, that is,

$$D_e = \max_{1 \leq i \leq N} |F(x_i) - F_t(x_i)| \ . \quad (6)$$

For each data set and each candidate distribution, D_e can be compared against the critical value D_{crit} associated with the chosen level of significance ($p < 0.05$) and the sample size (N). If D_e is greater than D_{crit} then the null hypothesis will be rejected and the data cannot plausibly be thought of as arising from the specified distribution. An alternative way to make this decision is to calculate the tail probability p corresponding to each observed D_e as obtained approximately by Press et al. (1992):

$$p = Q_{KS}((\sqrt{N} + 0.12 + 0.11/\sqrt{N}) D_e) \ , \quad (7)$$

where

$$Q_{KS}(x) = 2 \sum_{j=1}^{\infty} (-1)^{j-1} \mathrm{e}^{-2j^2x^2} \ . \quad (8)$$

If p calculated from (7) is less than 0.05 (the chosen significance level), then the null hypothesis can be rejected. Ideally, the parameters for the theoretical

functions should be estimated from data that are not from the sample used for the empirical CDF (Press et al. 1992), but this was not practical for the present paper.

5 Data analysis

Based on the algorithms described in the preceding sections, the parameters of each type of distribution were estimated for each of the 56 data sets. Figure 2 shows representative binocular rivalry perceptual dominance time series for three subjects, with two data sets shown for one of the subjects. Example dominance time series for the Necker cube are shown in Fig. 3. For the same examples, the empirical pdfs and fits of the three candidate theoretical distributions are shown in Fig. 4 (binocular rivalry) and Fig. 5 (Necker cube). Visual inspection (especially near the peaks) indicates that the lognormal distribution yields the best fit for all these examples.

The Kolmogorov–Smirnov one-sample goodness-of-fit test was performed to compare each of the 56

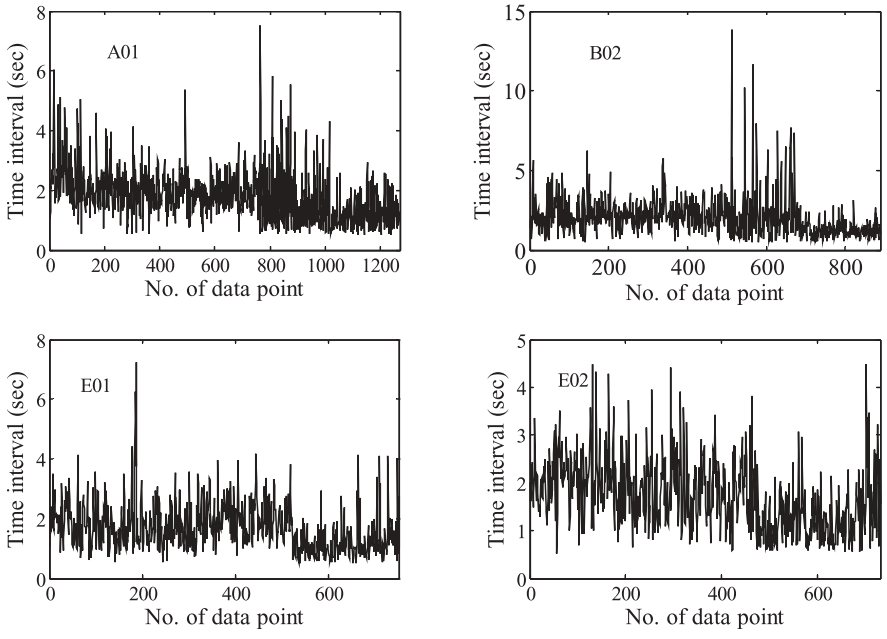

Fig. 2. Dominance time series for the binocular rivalry experiment (three subjects, but note that subject "E" has two time series shown)

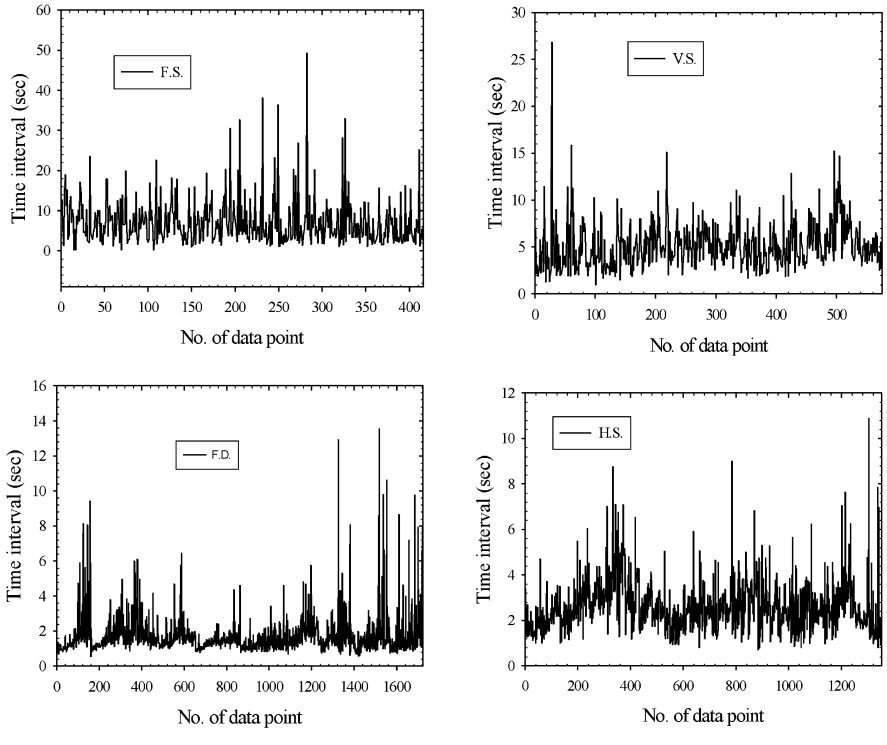

Fig. 3. Dominance time series for the Necker cube experiment (four subjects)

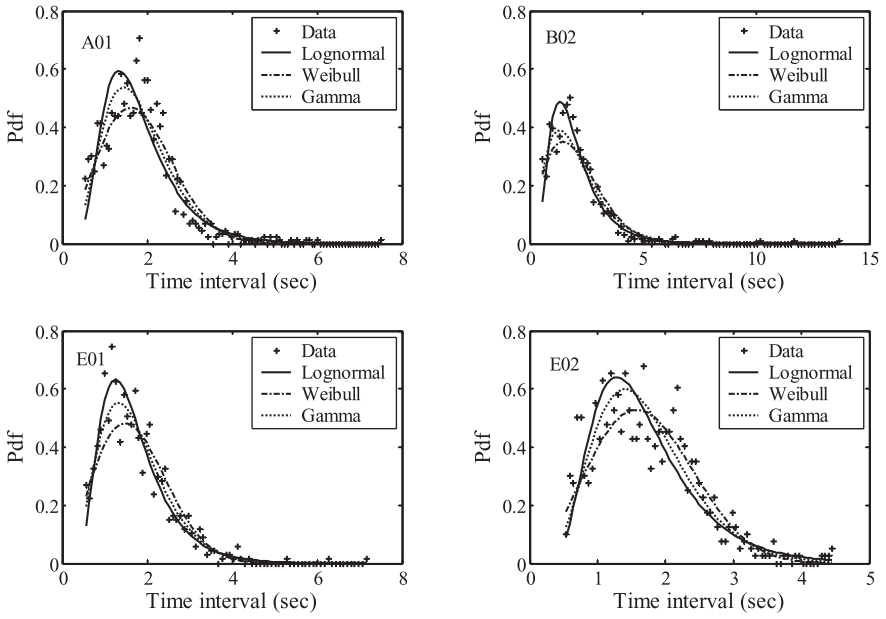

Fig. 4. Comparisons of empirical and theoretical probability density functions (pdfs) for binocular rivalry dominance times

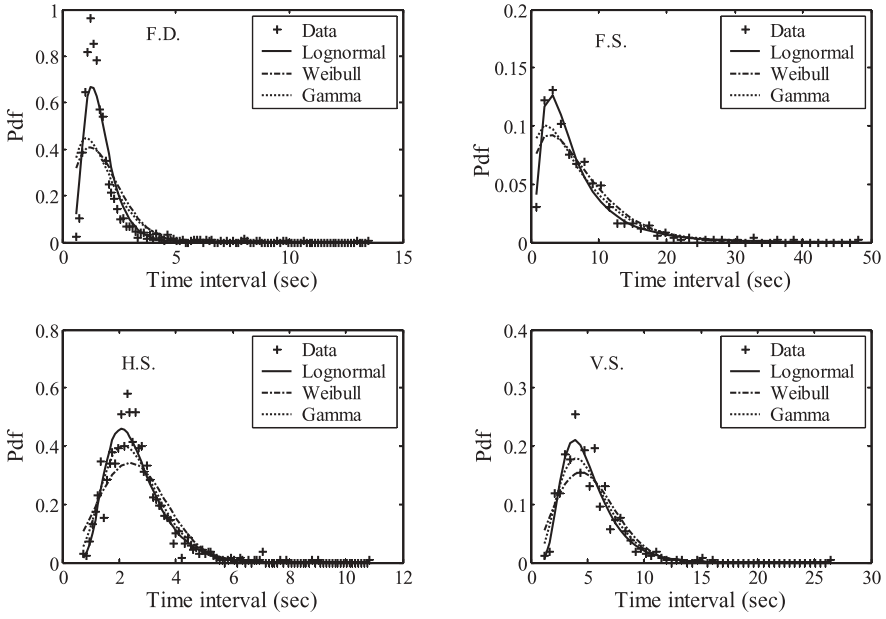

Fig. 5. Comparisons of empirical and theoretical probability density functions (pdfs) for Necker cube dominance times

empirical CDFs to each of the three theoretical candidate distributions (168 evaluations of (6–8)). Each of those evaluations resulted in a tail probability for the test statistic D_e, which served as the index of goodness-of-fit. Table 1 shows those goodness-of-fit indices for all multistable perception data series that passed the goodness-of-fit test, and Table 2 shows those indices of data series that failed in the test. Note that the results are sorted into groupings. In Table 1, we have 40 data sets in which subject ID B02 through Q01 represent results from the binocular rivalry experiments (std rivalry), R01 through Sub2 from binocular rivalry using the turning balls (ball rivalry) instead of gratings, Sub4 through Sub9 from the ambiguous motion turning ball (ambig motion), D.A. through V.S. from the Necker cube. In Table 2, we have 16 data sets in which subject ID A01 through N01 represent results from the binocular rivalry experiments, S01 and T01 from binocular rivalry using the turning balls instead of gratings, Sub3 from the ambiguous motion turning ball, A.F. through M.T. from the Necker cube. In Table 1, most likely outcomes (24 of 40 cases) were that the lognormal distribution plausibly fit the empirical pdfs, but the other two candidate distributions were rejected. The next most likely outcomes (9 of 40 cases) were both lognormal and gamma distributions plausibly fit the empirical pdfs (but not Weibull). Least likely outcomes were: (a) both lognormal and Weibull but not gamm distributions would give a plausible fits (4 of 40 cases), and (b) all three candidate distributions would give plausible fits (3 of 40 cases). Counting the 56 cases in the two tables, when a distribution was not rejected, ($p < 0.05$) yields 40 for

Table 1. Data sets passing the goodness-of-fit test for a lognormal distribution

Stimulus	ID	p (Weibull)	p (Lognormal)	p (Gamma)	N
Std rivalry	B02	< 0.001	**0.111**	0.010	889
Std rivalry	D01	< 0.001	**0.071**	< 0.001	802
Std rivalry	D02	< 0.001	**0.713**	0.040	787
Std rivalry	F01	< 0.001	**0.073**	0.014	628
Std rivalry	I02	0.025	**0.474**	0.041	343
Std rivalry	G02	< 0.001	**0.237**	< 0.001	589
Std rivalry	J01	< 0.001	**0.056**	< 0.001	1250
Std rivalry	J02	< 0.001	**0.326**	< 0.001	976
Std rivalry	K01	< 0.001	**0.108**	< 0.001	838
Std rivalry	O01	0.005	**0.914**	0.016	426
Std rivalry	P01	< 0.001	**0.712**	< 0.001	403
Ball rivalry	R01	0.038	**0.583**	< 0.001	670
Ball rivalry	U01	0.012	**0.278**	0.011	605
Ball rivalry	W01	0.006	**0.455**	< 0.001	591
Ball rivalry	X01	< 0.001	**0.564**	< 0.001	580
Ball rivalry	Z01	< 0.001	**0.369**	< 0.001	478
Ball rivalry	Sub2	0.027	**0.124**	0.011	469
Ambig motion	Sub4	0.003	**0.299**	< 0.001	400
Ambig motion	Sub5	0.017	**0.406**	< 0.001	385
Ambig motion	Sub6	0.004	**0.581**	< 0.001	379
Ambig motion	Sub9	0.008	**0.787**	< 0.001	307
Necker cube	H.S.	< 0.001	**0.060**	0.009	1353
Necker cube	J.C.	< 0.001	**0.070**	< 0.001	547
Necker cube	M.S.	< 0.001	**0.967**	0.002	620
Std rivalry	E01	0.021	**0.496**	**0.699**	753
Std rivalry	G01	0.009	**0.717**	**0.306**	532
Std rivalry	I01	0.037	**0.518**	**0.182**	439
Std rivalry	L01	0.039	**0.789**	**0.154**	695
Std rivalry	M01	0.028	**0.381**	**0.460**	632
Std rivalry	Q01	0.044	**0.751**	**0.246**	355
Ball rivalry	V01	0.038	**0.659**	**0.082**	591
Necker cube	D.A.	0.024	**0.317**	**0.056**	654
Necker cube	V.S.	0.011	**0.830**	**0.267**	575
Ball rivalry	Y01	**0.062**	**0.264**	0.030	525
Ball rivalry	Sub1	**0.072**	**0.772**	0.016	473
Ambig motion	Sub7	**0.084**	**0.222**	0.002	340
Necker cube	F.S.	**0.055**	**0.490**	0.009	416
Std rivalry	H01	**0.064**	**0.716**	**0.396**	448
Std rivalry	H02	**0.298**	**0.063**	**0.665**	486
Ambig motion	Sub8	**0.136**	**0.862**	**0.624**	339

Note: Bold font denotes satisfactory fit, that is, $p \geq 0.05$

Table 2. Data sets failing goodness-of-fit tests for a lognormal distribution

Stimulus	ID	p(Weibull)	p(Lognormal)	p(Gamma)	N
Std rivalry	A01	< 0.001	< 0.001	0.037	1269
Std rivalry	A02	< 0.001	< 0.001	0.008	1041
Std rivalry	B01	< 0.001	0.026	0.014	971
Std rivalry	C01	< 0.001	0.023	< 0.001	788
Std rivalry	C02	< 0.001	0.026	< 0.001	807
Std rivalry	F02	< 0.001	0.033	< 0.001	663
Ambig motion	Sub3	0.011	0.012	< 0.001	444
Necker cube	A.F.	< 0.001	0.020	< 0.001	937
Necker cube	F.D.	< 0.001	< 0.001	< 0.001	1724
Necker cube	H.K.	< 0.001	0.007	< 0.001	807
Necker cube	J.M.	< 0.001	< 0.001	< 0.001	1117
Std rivalry	N01	**0.968**	< 0.001	**0.094**	605
Ball rivalry	S01	**0.209**	0.044	**0.166**	665
Ball rivalry	T01	**0.104**	0.029	**0.372**	665
Std rivalry	E02	**0.170**	0.010	**0.096**	731

lognormal, 16 for gamma, and 11 for Weibull, and when three distributions were all rejected yields 12.

The error function can be used to compare empirical dominance time CDFs against the lognormal distribution (see (5)). Ideally, the data plotted in this fashion should be a straight line of unity slope when the fit is very good. This was true for the 40 cases of satisfactory lognormal fit given in Table 1. Figure 6 shows error

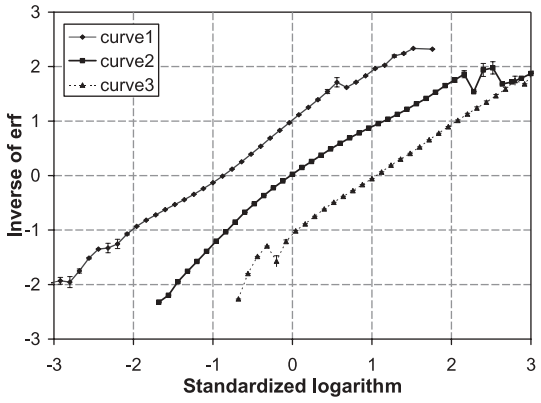

Fig. 6. Error functions plotted against lognormal standard scores for 15 time series that failed the lognormal distribution goodness-of-fit test. The data sets were grouped by inspection as follows. *Curve* 1 (platykurtic): A01, A02, B01, F02, N01, S01, T01, T01, Sub3, J.M.; *Curve* 2 (leptokurtic): A.F., F.D., H.K.; *Curve* 3 (leptokurtic and skewed): C01, C02, E02. Lines of different textures were displaced along the abscissa for clarity. *Error bars* illustrate standard deviations (across subjects), which are often smaller than the plotted points. An ideal lognormal distribution would yield a straight line with a slope of unity on this kind of plot

function plots for 15 of the cases combined into three groups that rejected the lognormal distribution, drawn from Table 2. Nine of those cases were similar in displaying a platykurtic pattern of deviations (observed frequencies too large near both ends of the distribution and too small near the mean). Curve 1 represents the average of these nine data sets, shifted one unit to the left on the abscissa for clarity. Error bars (± 1 standard deviation) are often smaller than the plotted points. Thus, undershoots near the mean and symmetrical overshoots near the two ends appear to be significant. Curve 2 represents the average of three cases drawn from Table 2 that were similar, displaying a leptokurtic pattern of deviations (observed frequencies too small near both ends of the distribution). Curve 3 represents the average of the last three cases drawn from Table 2 that were similar in displaying a leptokurtic and skewed pattern of deviations (observed frequencies too small near the negative but not the positive tail of the distribution); this curve shifted one unit to the right on the abscissa for clarity. Linearity is generally good near the middle of each plot (i.e., near the means of the empirical distributions). The discrepancies we find tend to happen most often either: (i) at the ends of Curves 1–3, where observations are more sparsely distributed and the low likelihood of occurrence is therefore difficult to estimate reliably, or (ii) in the middle of Curve 1, close to the mean, where the likelihood of occurrence can be estimated with better confidence. We believe that suitable fits even to these cases, which reject the lognormal fit, could be made by slight adjustment to the weight of the fourth moment (kurtosis) component.

6 Discussion

The lognormal distribution shape may have implications for mechanisms underlying multistable perception. In principle, if we consider perception to be a complex task composed of n independent subtasks, and the probability of success in the complex task is the product of the probabilities of all n subtasks succeeding, then task successes will have a lognormal distribution when n is sufficiently large to apply the central limit theorem. Leopold and Logothetis (1999) have proposed that perceptual multistability might be accidental consequences of rather general neural mechanisms that mediate a variety of behaviors, and this would seem to be consistent with the statistical principle above.

The lognormal distribution shape may also have implications for analysis of the time series dynamics. For example, Bershadskiiet al. (2001) have recently shown that the inter spike intervals of individual neurons can be plausibly explained by a thermodynamic model of cell membrane thresholds, resulting in a lognormal-like distribution of these time intervals as well as multifractal relationships in the higher-order statistics of their time series. Relationships of self-similarity in the spike trains are consistent with long-range correlations in their time series. All of these mathematically elegant features arose from their fundamentally simple thermodynamic premises. We have in fact followed the lead of Bershadskii et al. (2001) and of Gao and Rubin (2001) by applying monofractal and multifractal analysis to the time series of perceptual dominance responses. Our preliminary findings do, as expected, show indices of self-similarity (generalized Hurst parameters), indicative of long-range correlations in multistable perceptions (Gao et al. 2003).

References

Attneave F (1971) Multistability in perception. Sci Am 225:63–71

Bershadskii A, Dremencov E, Fukayama D, Yadid G (2001) Multifractal statistics and underlying kinetics of neuron spiking time-series. Phys Lett A 289:337–342

Blake R, Logothetis NK (2002) Visual competition. Nat Rev Neurosci 3:13–23

Bonneh Y, Gepshtein S (2001) Rivalry between alternative percepts of motion occurs within objects. In: Proceedings of the Vision Science Society meeting, Sarasota, FL, 4–8 May 2001, pp 229–235

Borsellino A, De Marco A, Allazetta A, Rinesi S, Bartolini A (1972) Reversal time distribution in the perception of visual ambiguous stimuli. Kybernetik 10:139–144

Crick F, Koch C (1990) Some reflections on visual awareness. Cold Spring Harb Symp Quant Biol 55:953–959

Ditzinger T, Haken (1990) The impact of fluctuations on the recognition of ambiguous patterns. Biol Cybern 63:453–456

Elbert T, Hommel J, Lutzenberger W (1985) The perception of Necker cube reversal interacts with the Bereitschaftspotential. Int J Psychophysiol 3:5–12

Gao J, Rubin I (2001) Multifractal modeling of counting processes of long-range dependent network traffic. Comput Commun 24:1400–1410

Gao JB, Merk I, Tung WW, Billock V, White KD, Harris JG, Roychowdhury VP (2003) Persistence and 1/f spectra in multistable visual perception. Phys Rev Lett (in press)

Gómez C, Argandoa ED, Solier RG, Angulo JC, Vázquez M (1995) Timing and competition in networks representing ambiguous figures. Brain Cogn 29:103–114

Haken H (1994) A brain model for vision in terms of synergetics. J Theor Biol 171:75–85

Inui T, Tanaka S, Okada T, Nishizawa S, Katayama M, Konishi J (2000) Neural substrates for depth perception of the Necker cube: a functional magnetic resonance imaging study in human subjects. Neurosci Lett 282:145–148

Kennedy JB, Neville AM (1986) Basic statistical methods for engineers and scientists. 3rd edn. Harper& Row, Publishers, Inc., New York

Kruse P, Carmesin HO, Pahlke L, Strüber D, Stadler M (1996) Continuous phase transitions in the perception of multistable visual patterns. Biol Cybern 75:321–330

Laing CR, Chow CC (2002) A spiking neuron model for binocular rivalry. J Comput Neurosci 12:39–53

Lehky SR (1995) Binocular rivalry is not chaotic. Proc R Soc Lond B Biol Sci 259(1354):71–76

Leopold DA, Logothetis NK (1999) Multistable phenomena: changing views in perception. Trends Cogn Sci 3:254–264

Leopold DA, Wikle M, Maier A, Logothetis NK (2002) Stable perception of visually ambiguous patterns. Nat Neurosci 5:605–609

Lumer ED, Friston KJ, Rees G (1998) Neural correlates of perceptual rivalry in the human brain. Science 280:1930–1934

Merk I, Schnakenberg J (2002) A stochastic model of multistable visual perception. Biol Cybern 86:111–116

Miller I, Freund JE (1985) Probability and statistics for engineers. 3rd edn. Prentice-Hall, Englewood Cliffs, NJ

Nagao N, Nishimura H, Matsui N (2000) A Neural chaos model of multistable perception. Neural Processing Lett 12:267–276

Otterpohl JR, Haynes JD, Emmert-Streib F, Vetter G, Pawelzik K (2000) Extracting the dynamics of perceptual switching from 'noisy' behaviour: an application of hidden Markov modeling to pecking data from pigeons. J Physiol (Paris) 94:555–567

Pettigrew JD, Miller SM (1998) A 'sticky' interhemispheric switch in bipolar disorder? Proc R Soc B 265:2141–2148

Press WH, Teukolsky SA, Vetterling WT, Flannery BP (1992) Numerical recipes in FORTRAN: the art of scientific computing, 2nd edn. Cambridge University Press, Cambridge

Sengpeil F (2000) An alternative view of perceptual rivalry. Curr Biol 10:R482–R485

Siegel S (1956) Non-parametric statistics for the behavioral sciences. McGraw-Hill, New York

Sterzer P, Russ MO, Preibisch C, Kleinschmidt A (2002) Neural correlates of spontaneous direction reversals in ambiguous apparent visual motion. Neuroimage 15:908–916

Tong F, Nakayama K, Vaughan JT, Kanwisher N (1998) Binocular rivalry and visual awareness in human extrastriate Cortex. Neuron 21:753–759

Vetter G, Haynes JD, Pfaff S (2000) Evidence for multistability in the visual perception of pigeons. Vision Res 40:2177–2186

von Steinbüchel N (1998) Temporal ranges of central nervous processing: clinical evidence. Exp Brain Res 123:220–233

White KD, Leonard CM, Kuldau JM, Bengtson M, Ricciuti N, Maron L, Mahoney B, Pettigrew JD (2002) Perceptual stability at high rates of dichoptic stimulus alternation in schizophrenia. J Neurosci (in press)

Wilson HR, Krupa B, Wilkinson F (2000) Dynamics of perceptual oscillations in form vision. Nat Neurosci 3:170–176